Available online at www.sciencedirect.com
SCIENCE DIRECT
Catalysis Today 114 (2006) 13–22
CATALYSIS TODAY
www.elsevier.com/locate/cattod

NO_x SCR by decane and propylene on Pt + Cu/Zr-pillared clays in realistic feeds: Performance and mechanistic features versus structural specificity of nanosized zirconia pillars

Vladislav Sadykov [a,*], Tatiana Kuznetsova [a], Vladimir Doronin [a], Rimma Bunina [a], Galina Alikina [a], Lubsan Batuev [a], Valerii Matyshak [b], Aleksander Rozovskii [c], Valentin Tretyakov [c], Tatiana Burdeynaya [c], Valerii Lunin [d], Julian Ross [e]

[a] *Boreskov Institute of Catalysis SB RAS, Pr. Lavrentieva 5, 630090 Novosibirsk, Russia*
[b] *Semenov Institute of Chemical Physics RAS, Moscow, Russia*
[c] *Topchiev Institute of Petrochemical Synthesis RAS, Moscow, Russia*
[d] *Chemical Department of Lomonosov Moscow State University, Moscow, Russia*
[e] *The Limerick University, Limerick, Ireland*

Abstract

Pt + Cu-loaded ZrPILC tested in the reactions of NO_x selective catalytic reduction by propylene and decane in realistic feeds with a high content of water, oxygen and an admixture of SO_2 demonstrated promising performance at high space velocities (up to 100 000 h^{-1}) in the temperature range of 150–400 °C. A strong promoting effect of water, oxygen and the catalyst presulfation on the degree of NO_x conversion into N_2 was revealed. The specificity of these catalyst action in realistic feeds was explained by taking into account the textural, structural and surface features of zirconia-pillared clays as well as the mechanism of NO_x HC SCR reaction including participation of strongly bound species in key stages.

Keywords: Diesel exhausts; de-NO_x by HC SCR; Zirconia-pillared clays; Supported Pt + Cu; Performance in realistic feeds; Presulfation; Mechanism of action by in situ FTIRS

1. Introduction

Selective catalytic reduction of nitrogen oxides by hydrocarbons in lean-burn conditions (NO_x HC SCR) could be a promising option for NO_x abatement from the diesel exhausts [1]. This requires design of catalysts possessing a high hydrothermal stability and able to operate at rather low (200–400 °C) temperatures in the presence of sulfur dioxide and water in the feed. Diesel fuel or products of its partial oxidation (olefins [1], oxygenates [2,3]) are the most attractive reductants due to their high reactivity and availability/possibility to be produced on-board via the partial oxidation of diesel fuel [3]. Catalysts are thus required to be moderately acidic and hydrophobic to prevent their excessive sulfation, coking and water condensation in pores in humid feeds [2]. Though zeolitic systems meet these demands, they are not hydrothermally stable and suffer from the activity loss due to dealumination and active components (such as copper cations) aggregation [4]. Alumina-supported promoted silver [5] or Pt [6] catalysts as well as transition metal cations on sulfated zirconia [7–9] are not sufficiently active in the temperature range of real diesel exhausts (200–400 °C) in the presence of sulfur dioxide in the feed.

Catalysts based upon zirconia-pillared montmorillonite clays (ZrPILC) [10] appear to be promising for considered application. Indeed, the structural unit of these clays comprised of the Al–(Me^{2+})–O octahedral layer sandwiched between two SiO_4 layer is inherently hydrophobic and stable to sulfation. Nanosized zirconia pillars propping the clay sheets create galleries with typical sizes in the ultramicropore range [11]. Earlier, these catalysts with supported Pt + Cu were shown to be reasonably active in NO_x SCR by propane, propylene and

* Corresponding author.
E-mail address: sadykov@catalysis.nsk.su (V. Sadykov).

0920-5861/$ – see front matter
doi:10.1016/j.cattod.2006.02.010

decane in dry feeds [12–15]. Moreover, sulfation of zirconia is known to increase its acidity. This facilitates hydrocarbons activation into oxygenates and improves supported transition metal cation activity and selectivity in NO_x HC SCR [7–9,16,17], while hindering formation of H–N–C–O deposits detrimental to the catalyst performance [18]. The same positive features were expected for the case of Zr-PILC-based catalysts as well.

This work presents results on the characterization of catalytic properties of Pt + Cu-loaded zirconia-pillared clays in the reaction of NO_x selective reduction by decane or propylene at high space velocities in realistic feeds with a big content of oxygen, water and an admixture of sulfur dioxide. A high performance of these catalysts in the low- and middle-temperature range was indeed observed and explained with a due regard for their texture [11,19], structure of zirconia nanopillars and supported active components [12,13,19] as well as features of the reaction mechanism involving steps with participation of strongly bound nitrates, organic oxygenates and nitrocompounds elucidated with the help of in situ FTIR studies [20].

2. Experimental

Synthesis of samples of zirconia-pillared clays (zirconia content ~20 wt.%) has been carried out using a Ca-montmorillonite clay (initial CaO content 2 wt.%; Fe admixture content ~0.2 wt.%) according to optimized procedures of pillaring with $ZrOCl_2$ solution aged with addition of $CaCl_2$ as described in details elsewhere [12,13]. After pillaring and washing procedure, the residual content of Ca in pillared clay was found to be below 0.2 wt.%. After calcination at 500 °C, a sample of ZrPILC used in this work is characterized by the BET specific surface area of 265 m^2/g, a developed pore structure (the integral pore volume up to 0.25 cm^3/g, micropore volume 0.17 cm^3/g, the average slit-like micropore size ~0.8 nm, the average mesopore size ~5 nm [19]). Cu (~2 wt.%) and/or Pt (0.3 wt.%) were supported by the incipient impregnation with the water solutions of Cu nitrate and H_2PtCl_6, respectively, followed by drying and calcination at 500 °C. For comparison, the same amounts of copper and Pt were supported by the identical procedure on the bulk mesoporous zirconia sample (specific surface area 180 m^2/g) stabilized by addition of 3.3 wt.% Ca [21]. For the same purpose, samples containing 0.5 wt.% Pt were prepared by the incipient wetness impregnation of an industrial A-1 γ-Al_2O_3 support (specific surface area 180 m^2/g) or alumina-pillared montmorillonite clay (the specific surface area and pore structure parameters being close to those of ZrPILC [22]) with H_2PtCl_6 solution followed by drying and calcinations at 500 °C.

Sulfation of Pt or Pt + Cu-loaded samples was carried out following earlier described procedures [23–27] by impregnation with $(NH_4)_2SO_4$ solutions followed by drying and calcinations at 500 °C. In all cases, the sulfur content was kept at about 1 wt.% S as determined by the chemical analysis.

The temperature-programmed desorption (TPD) of NO_x from the surface of samples after oxidative pretreatment (1 h, 400 °C, 10% O_2 in He flow) was carried out with the temperature ramp from 25 to 550° at 10°/min rate using a PEM-2M IR absorption NO_x analyzer for NO and NO_2 monitoring. NO_x was adsorbed from the mixture of NO (0.1%) + O_2 (2.5%) in He at room temperature for 1 h followed by the He purging for removing all physisorbed species before the TPD run. To check the effect of sample hydroxylation on the NO_x TPD spectra, after cooling to room temperature in the flow of 10% O_2 in He mixture, before NO_x adsorption, sample was kept for 0.5 h in the flow of He saturated with the water vapor by bubbling it through the saturator at a room temperature.

The properties of catalysts in the NO_x HC SCR reactions were tested in flow microreactors following previously described procedures [12–14,21] at space velocities (GHSV) varying in the range of 10 000–90 000 h^{-1} using propylene and decane as reductants. While NO content in the feed was kept at 0.05–0.2% level, the oxygen content was varied in the range of 1–10%, H_2O: 0–10%, SO_2: 0–300 ppm. After passing through a cooler kept at 20 °C to remove the excess of water, reaction mixtures were continuously analyzed by a PEM-2M infra-red absorbance analyzer for CH_x, NO, NO_2, CO, and CO_2. In addition, GC equipped with a thermal conductivity detector and columns filled with NaX and Polysorb (He being the carrier gas) was used for the periodic control of N_2, O_2, CO, CO_2 and N_2O. The error in determining NO_x conversions by the infra-red analyzer was found to be ca. 5 rel.%. At a high (~10%) content of oxygen in the feed, due to overlapping of chromatographic N_2 and O_2 peaks, the value of the NO_x conversion into N_2 was estimated from the decrease of NO_x content in the reaction mixture and concentration of formed N_2O. In all studied cases, for Pt + Cu/ZrPILC catalysts, NO_2 content in the converted mixture was quite low even in feeds with a big content of oxygen decreasing from ~50 to 10 ppm in the temperature range of 200–450 °C. Decane conversion was usually estimated from the content of CO_2 in the products, since for studied catalysts and experimental conditions, CO was not observed. For feeds with a big oxygen and water content, the error in estimation of decane conversions, especially in the low-temperature range, could be rather big, due to possible formation of oxygenates not analyzed by GC and CO_2 (along with oxygenates) removal with the water condensed in the cooler.

The in situ Fourier transform infra-red (FTIR) spectra in the course of components adsorption, desorption and/or reaction were recorded in the transmission mode using a Perkin-Elmer "Spectrum RX I FTIR System" spectrometer and a specially designed flow cell [28].

3. Results

3.1. Effect of support and the active component

As follows from the typical data shown in Fig. 1, for reaction mixtures with sufficiently high oxygen content, at a close performance in the decane oxidation, conversion of NO_x is higher for Pt + Cu/ZrPILC catalyst than for Pt/alumina catalyst. Moreover, for the latter catalyst, in this feed, in the temperature

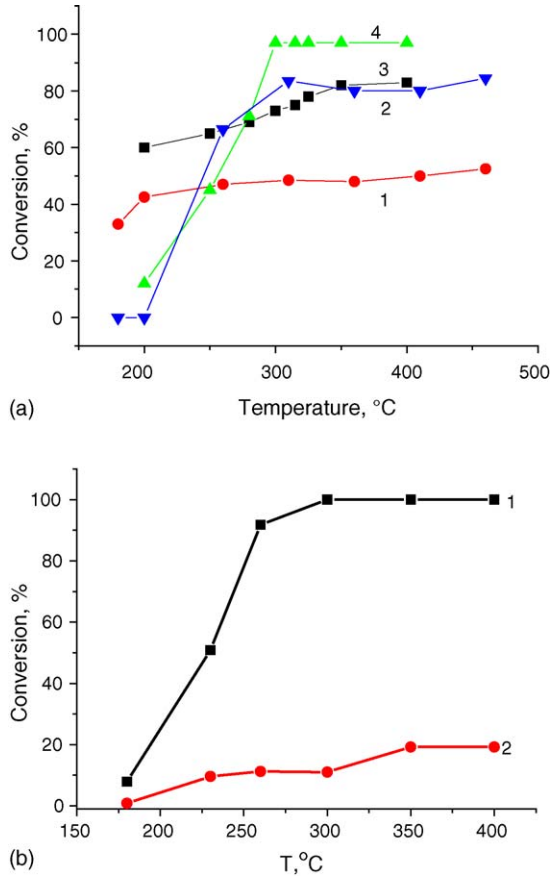

Fig. 1. (a) Temperature dependence of NO_x (1, 3) and decane (2, 4) conversions for 0.5% Pt/Al_2O_3 (1, 2) and Pt + Cu/ZrPILC (3, 4) catalysts. Reaction mixture composition 0.1% NO + 0.05% $C_{10}H_{22}$ + 1% H_2O + 10% O_2 in He, GHSV 30 000 h^{-1}. (b) Temperature dependence of decane (1) and NO_x (2) conversions for 0.3 wt.% Pt + 2 wt.% Cu/Ca–ZrO_2 catalyst. Reaction mixture composition 0.05% NO + 0.05% $C_{10}H_{22}$ + 1.2% H_2O + 5% O_2 in He, GHSV 12 500 h^{-1}.

range of 200–300 °C, selectivity of NO_x conversion into N_2O is around 75%, while it is below 20% for Pt + Cu/ZrPILC catalyst. Hence, presence of copper in the mixed active component allows to decrease generation of undesired by-product –N_2O thus overcoming the main drawback of supported Pt catalysts [23,29,30]. For both catalysts, apparent underestimation of decane conversion in the low-temperature range seems to be explained both by a big error in its evaluation (vide supra) and potential ability of one decane molecule to reduce up to 15.5 NO_2 (31 NO) molecules.

For Pt-supported onto alumina-pillared clay, in the same feed, even at a lower (12 500 h^{-1}) GHSV, NO_x conversion was found to be around 20–30% in the temperature range 250–500 °C (not shown for brevity). Hence, by itself, alumosilicate supports based upon the natural aluminosilicates—montmorillonite clays could not provide a high efficiency of supported Pt in NO_x decane SCR.

Earlier [12,31], for Cu cations supported onto ZrPILC without other promoters, in the feed containing 500 ppm of decane and 1500 ppm of NO_x in air (GHSV 13 000 h^{-1}), in the same temperature range, NO_x conversion was found to be ~10–20%. Hence, promotion of Cu/ZrPILC catalyst by Pt allowed to strongly enhance its performance in NO_x decane SCR in the oxygen excess.

For 3.7 wt.% Cu supported onto bulk zirconia oxide (monoclinic phase), in the feed containing 9% O_2 in the mixture with NO and decane, at GHSV 70 000 h^{-1}, the maximum level of NO reduction into N_2 was ~20% at ~275 °C, while only NO_2 was formed at temperatures exceeding 450 °C [8]. NO_x conversions ~15% at 300 °C and ~38% at 500 °C were obtained for the catalyst comprised of 5 wt. CuO supported on Ca-stabilized cubic mesoporous ZrO_2 (feed 500 ppm of decane and 1500 ppm of NO_x in air, GHSV 11 200 h^{-1} [21]. In contrary to ZrPILC, performance of copper cations supported onto this bulk zirconia was not improved by adding Pt (Fig. 1b), though decane combustion efficiency was apparently high. For this sample, N_2O formation was not observed suggesting negligible participation of Pt in the NO_x selective reduction by decane.

Hence, in feeds with a realistic oxygen content, NO_x selective reduction into N_2 by decane proceeds more efficiently and selectively for the catalyst based upon zirconia-pillared clay with supported Pt + Cu mixed active component.

3.2. Effect of the feed composition

Fig. 2 demonstrates that in a dry feed with the minimum excess of oxygen, NO_x conversion in decane SCR on Cu + Pt/ZrPILC catalyst is much lower than in the realistic feed, while N_2O is mainly formed. A low degree of decane conversion suggests that the catalyst is heavily coked, which is confirmed by visual blackening of the discharged catalyst. At low temperatures, on the partially coked catalyst, NO_x transformation into N_2O in the dry feed could proceed on Pt sites via the decomposition route [29], while Cu cations appear to play a minor role. At high (~400 °C) temperatures, coke oxidation by NO_2 along with O_2 could generate NO therefore decreasing the overall NO to N_2 conversion. In the realistic feed, at a much higher space velocity, a high degree of NO_x conversion with complete absence of N_2O in products (Fig. 2) implies operation of another NO_x HC SCR route.

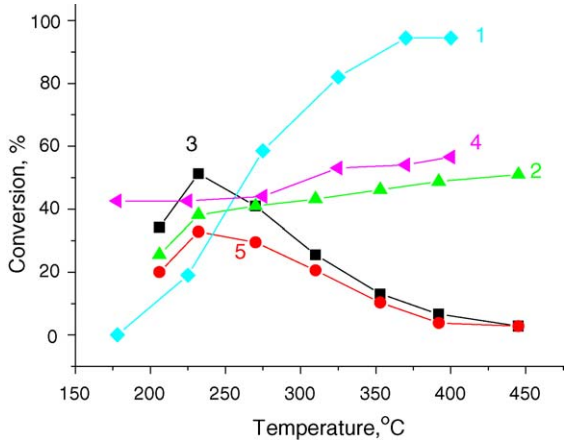

Fig. 2. Decane (1, 2) and NO_x conversion versus temperature into $N_2 + N_2O$ (3), N_2 (4) and N_2O (5) in $C_{10}H_{22}$ SCR on Pt + Cu/ZrPILC. (1, 4) Feed 0.1% NO + 0.05% $C_{10}H_{22}$ + 10% H_2O + 10% O_2 + 300 ppm SO_2, GHSV 90 000 h^{-1}; (2, 3, 5) feed 0.1% NO + 0.05% $C_{10}H_{22}$ + 1.5% O_2 + in He, GHSV 12 500 h^{-1}.

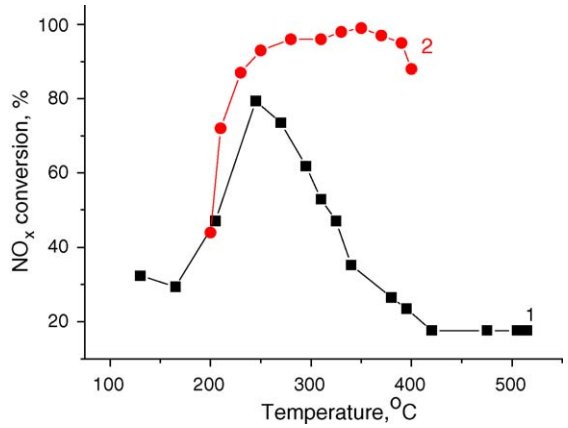

Fig. 3. NO_x conversion vs temperature in C_3H_6 SCR on Pt + Cu/ZrPILC. (1) 0.2% NO + 0.2% C_3H_6 + 2.5% O_2 in N_2, GHSV 30 000 h^{-1}. (2) 0.2% NO + 0.2% C_3H_6 + 2.5% O_2 + 200 ppm SO_2 + 3% H_2O in N_2, GHSV 70 000 h^{-1}.

In the reaction of NO_x SCR by propylene (Fig. 3), similar effects were observed when a dry feed was replaced by a more realistic one. Here, due to a higher reactivity of propylene, its complete combustion in the dry feed was observed at ~250 °C, while a rather high NO_x conversion was obtained. This implies a much lower degree of the catalyst coking by propylene in the dry feed used in this experiment. While for the dry feed N_2O formation was observed in a narrow temperature range 250–300 °C (maximum N_2O selectivity ~20%), it was completely absent for feeds with a high content of water and oxygen. Though in this case the increase of the maximum NO_x conversion for the realistic feed is not so impressive as in Fig. 2, a broad temperature range of the efficient performance achieved at a higher GHSV is worth noting. Hence, for both types of reductants, in realistic feeds, performance of Pt + Cu/ZrPILC catalyst is greatly improved suggesting similar reasons for this phenomenon.

Fig. 4 shows that in decane NO_x SCR, both water and oxygen are required for the high efficiency of NO_x conversion into N_2. Apparently, oxygen is more important for ensuring a high level of NO_x conversion at both low and high temperatures. This can be assigned to a higher rate of NO conversion into reactive intermediates—NO_2 and nitrite–nitrate species [20] at a big oxygen content in the feed. Decane conversion into deep oxidation products (CO_2) is less sensitive to the feed composition provided either water or oxygen are in a great excess which apparently helps to suppress coking. Thus, at 350 °C, decane conversion is ~60% for all feed compositions, being higher at higher and lower temperatures for feeds with a big oxygen content.

As follows from Fig. 5, SO_2 addition to the feed with a big content of water and oxygen allows to achieve a high level of NO_x conversion at higher GHSV. The increase of the space velocity is expected to decrease the degree of SO_2 oxidation into SO_3, thus decreasing the extent of the surface sulfation. As the result, the most pronounced increase of NO_x conversion (up to ~60%) in SO_2-containing mixture was observed at 40 000 h^{-1} GHSV (not shown for brevity). For this feed, N_2O formation was completely suppressed. At temperatures below 300 °C, a somewhat lower decane conversion in the SO_2-containing feed at nearly identical values of NO_x conversion implies a higher selectivity of hydrocarbon consumption for NO_x SCR. As was suggested by Figueras et al. for the case of Cu/sulfated zirconia catalyst [7,8], this can be explained by a higher selectivity of decane oxidation into such intermediates as oxygenates favored by a higher surface acidity.

Similar effects of SO_2 addition to the feed were observed for Pt-supported ZrPILC (not shown for brevity). At fixed (30 000 h^{-1}) GHSV, SO_2 addition to the feed containing 10% H_2O and 10% O_2 in the mixture with decane and O_2 increases NO_x conversion at 250 °C from ~20 to 50% while decreasing N_2O selectivity from ~50 to 20%. Earlier, improvement of N_2 selectivity for Pt on B_2O_3–SiO_2–Al_2O_3 or $AlPO_4$ supports due to addition of SO_2 to the feed was also observed by Zhang et al. [23] for NO_x C_3H_6 SCR.

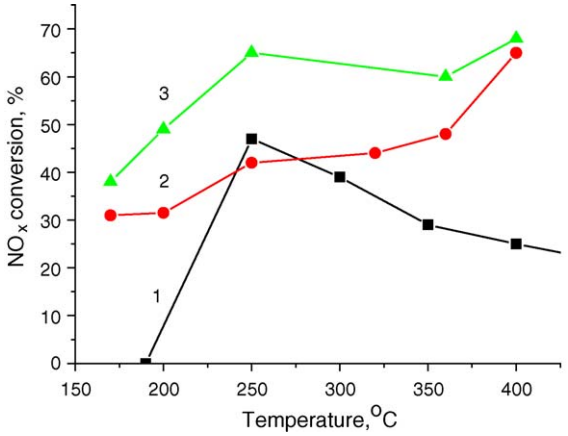

Fig. 4. Effect of H_2O and O_2 content in the feeds containing 0.1% NO and 0.05% $C_{10}H_{22}$ in He on NO_x conversion for Pt + Cu/ZrPILC catalyst. (1) 10% H_2O + 2% O_2; (2) 1% H_2O + 10% O_2; (3) 10% H_2O + 10% O_2. GHSV 50 000 h^{-1}.

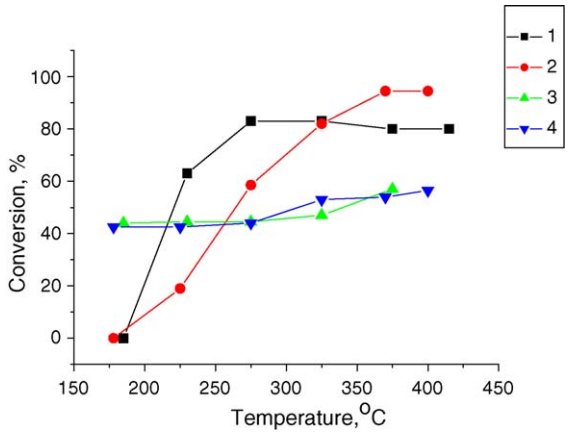

Fig. 5. Effect of sulfur dioxide (300 ppm) addition to the reaction mixture containing 0.1% NO + 0.05% $C_{10}H_{22}$ + 10% H_2O + 10% O_2 in He on decane (1, 2) and NO_x (3, 4) conversion on Pt + Cu/ZrPILC catalyst. GHSV 30 000 h^{-1} (1, 3) for feed without SO_2 and 90 000 h^{-1} (2, 4) for feed with 300 ppm SO_2.

3.3. Effect of the catalyst presulfation

The Pt + Cu/ZrPILC catalyst presulfation (Fig. 6) results in a stable improvement of both decane and NO_x conversion efficiency. Sulfation of Cu/ZrPILC catalyst (not shown for brevity) decreases decane conversion, while only slightly affecting NO_x conversion. Sulfation of bulk zirconia with supported transition metal cations also results in suppressing combustion of hydrocarbons, thus improving NO_x reduction selectivity [7–9,16,26]. Hence, a higher rate of decane oxidation for sulfated Pt + Cu/ZrPILC sample can be assigned to the effect of Pt in the complex active component (vide supra). Note that for Cu/sulfated zirconia [7,9], at comparable space velocity (70 000 h^{-1}), a detectable degree of NO_x conversion was observed only at temperatures exceeding 250 °C. Hence, presence of Pt in sulfated Pt + Cu/ZrPILC sample is at least one of the factors determining a high level of its low-temperature activity in NO_x decane SCR.

3.4. NO_x TPD

NO_x TPD spectrum for oxidized Pt + Cu/ZrPILC sample contains peaks of NO and NO_2 evolution (Fig. 7) which can be assigned to decomposition of different surface complexes including nitrosyl, nitrite and nitrate species [13,20,22,27,32]. In these adsorption conditions, N_2O_3 or adsorbed HNO_2 fixed at Zr^{4+} cations could exist as well [22]. The integral coverage of the surface by all ad-NO_x species does not exceed 1% of monolayer as related to the overall pillared clay surface. As was demonstrated earlier [13], supporting of Pt on Cu/ZrPILC results in decreasing the surface coverage by strongly bound nitrate species and facilitating their thermal decomposition as expressed by the low-temperature shift of the corresponding peaks of NO evolution.

Hydroxylation of the Pt + Cu/ZrPILC results in disappearance of the low-temperature peak corresponding to decomposition of nitrosyls or N_2O_3 species (Fig. 7). Instead, the overall amount of NO desorbed in the range up to 550 °C

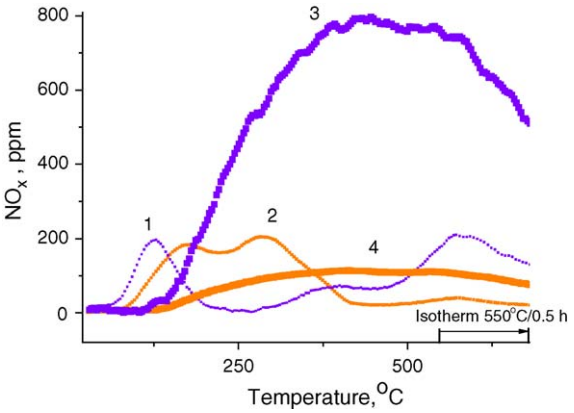

Fig. 7. Effect of the catalyst hydration on NO_x TPD spectra for Pt + Cu/ZrPILC catalyst. (1, 3) NO; (2, 4) NO_2. (1, 2) Pretreatment in dry O_2, (3, 4) pretreatment in O_2 followed by the catalyst hydration by water-saturated He stream.

increases, while the amount of desorbed NO_2 remains practically constant. Condensation of water in supermicropores of zirconia-pillared clays forms a film of the liquid phase in which N_2O_3 (NO NO_2) oxide can be dissolved. Hence, by analogy with the results of Sun et al. [33], increased amount of ad-NO_x species for hydrated ZrPILC can be assigned to hydration of N_2O_3 yielding HONO acid. Decomposition of this acid concomitant with the water desorption occurs in a broad temperature range. At a high (10–20%) water content in the feed, HNO_2 can be retained within micropores even at higher temperatures. Incorporation of the acid molecules into the defect positions of the aluminosilicate sheets could not be excluded as well.

Sulfation of Pt + Cu/ZrPILC sample decreases the amount of surface nitrates and their thermal stability (Fig. 8), which agrees with similar results of Kantcheva et al. [17,24,25] for sulfated bulk zirconia with or without supported Co cations. This is explained by adsorption of sulfates on zirconia nanopillars partially displacing nitrates. Some copper cations are covered by sulfates as well, while retention of sulfates on Pt is hardly probable.

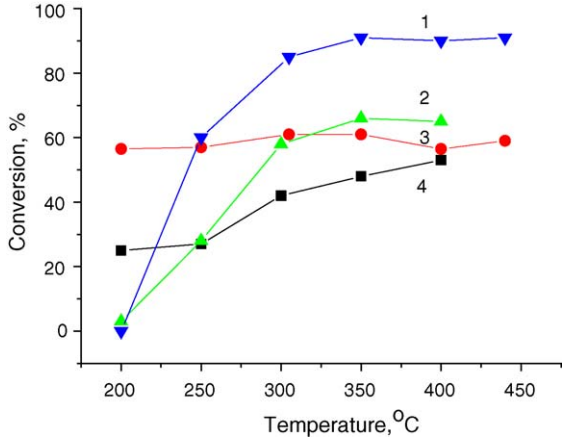

Fig. 6. Effect of Pt + Cu/ZrPILC catalyst sulfation on the decane (1, 2) and NO_x (3, 4) conversion at GHSV 30 000 h^{-1} and feed composition 0.1% NO + 0.05% $C_{10}H_{22}$ + 10% H_2O + 10% O_2 in He. (1, 3) Sulfated catalyst; (2, 4) before sulfation.

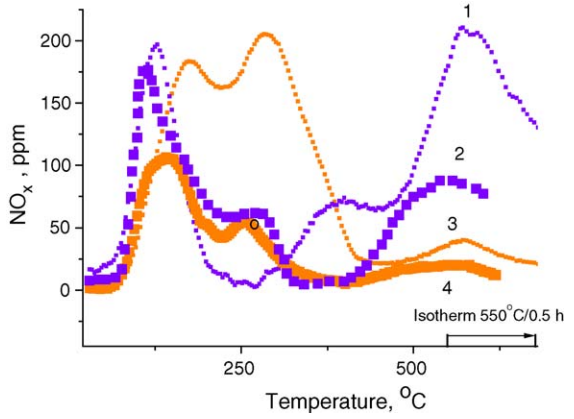

Fig. 8. Effect of sulfation on the NO_x TPD spectra of Pt + Cu/ZrPILC catalyst. (1, 2) NO; (3, 4) NO_2. (1, 3) Initial catalyst; (2, 4) after sulfation.

3.5. Nature and reactivity of the surface species in NO_x propylene SCR

Independent of the presence of supported Pt + Cu, at relatively low temperatures, under contact with $C_3H_6 + O_2$ mixture, propylene is first transformed into isopropoxide complex revealed by bands at 1394, 1381 cm^{-1} (δ-CH_3); 1460 cm^{-1} (δ_{as}-CH_3); 1335 cm^{-1} (δ_s-CH_3), 2980, 2920 and 2880 cm^{-1} (νC–H) [34]. Since formation of isopropoxide is accompanied by the decrease of the intensity of hydroxyl groups bands (3620–3740 cm^{-1} range), this suggests their participation in the propylene activation. Subsequent transformation of these complexes in the presence of oxygen leads to formation of coordination bound acetone (bands at 1670 cm^{-1} (νC=O), 1420 cm^{-1} (δ_{as}-CH_3), 1370 cm^{-1} (δ_s-CH_3) and 1250 cm^{-1} (νC–C)) and acetate (bands at 1555 cm^{-1} ($\nu_{as}COO^-$) and 1445 cm^{-1} (ν_sCOO^-)) complexes [34]. For Pt + Cu-loaded sample, linear and bridging carbonyls located on Pt atoms (bands at 2047 and 1830 cm^{-1}, respectively) are observed as well.

When NO is present in the mixture with C_3H_6 ($C_3H_6 + O_2$), at temperatures of catalysis, along with bands corresponding to bridging (1617 and 1257 cm^{-1}) and bidentate (1588 and 1248 cm^{-1}) nitrates [20], a set of bands assigned to a nitroorganic (the most probably dinitropropane [35]) complex (ν_sNOO at 1575 cm^{-1} and ν_{as}NOO at 1386 cm^{-1}; δC–H at 1435 and 1340 cm^{-1}; νC–H at 2730, 2887, 2945 and 2985 cm^{-1}) is observed. Bands corresponding to isocyanate (2236 cm^{-1}) and NH_x (3160 cm^{-1}) [34] species were detected as well, suggesting their participation in the reaction route. Detected intermediates are similar to those usually considered in the general NO_x HC SCR reaction scheme for the oxide catalysts [20,29,36].

Typical in situ FTIR experiments illustrating the dynamics of the surface species transformation under contact with the gas-phase components are presented in Figs. 9 and 10. As follows from Fig. 9, bidentate nitrates-dominating ad-NO_x species for ZrPILC at studied temperatures [20] are consumed by the reaction with $C_3H_6 + O_2$ mixture yielding dinitropropane along with oxygenates. Similarly (Fig. 10), isopropoxide reacts with $NO + O_2$ mixture giving dinitropropane along with acetone.

Estimation of the rate constants of nitrates transformation in these experiments as well as corresponding steady-state surface coverages by nitrates using earlier described approaches [20] allowed to calculate the rates of corresponding stages for ZrPILC and Pt + Cu/ZrPILC and compare them with the rates

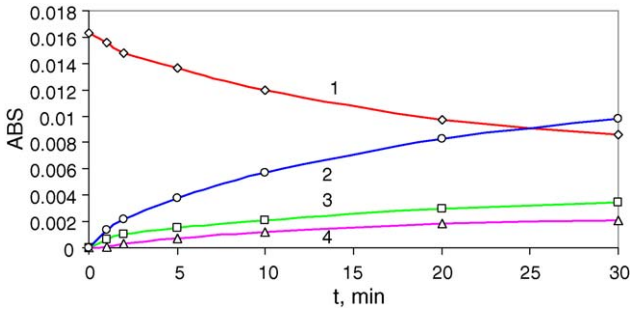

Fig. 9. Intensity of the surface species IR bands versus time of nitrate complexes titration by propylene (0.2%) + oxygen (2.5%) mixture in N_2 at 250 °C. (1) Bidentate nitrate (1616 cm^{-1}); (2) acetone (1670 cm^{-1}); (3) dinitropropane (1387 cm^{-1}); (4) isopropoxide (1394 cm^{-1}). Nitrates were preformed on the surface of ZrPILC by contact with NO (0.2%) + O_2 (2.5%) in N_2 at 250 °C.

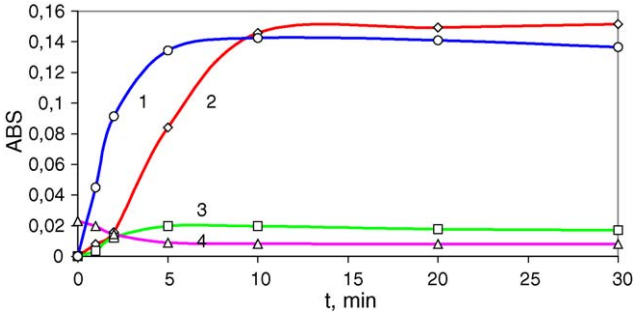

Fig. 10. Intensity of the surface species IR bands vs. time of isopropoxide complexes titration by NO (0.2%) + oxygen (2.5%) mixture in N_2 at 100 °C. (1) Acetone (1670 cm^{-1}); (2) bidentate nitrate (1616 cm^{-1}); (3) dinitropropane (1387 cm^{-1}); (4) isopropoxide (1394 cm^{-1}). Isopropoxide complexes preformed on the surface of ZrPILC by contact with C_3H_6 (0.2%) + O_2 (2.5%) in N_2 at 100 °C.

of steady-state catalytic reactions (Table 1). A good agreement between these rates proves that nitrates are key intermediates, and their transformation is the rate-determining stage of the catalytic reaction. However, close values of the rate constant for the stage of dinitropropane transformation under the $NO + O_2$ mixture effect (Table 1) imply that catalytic reaction can be controlled both by the stage of nitrates consumption leading to generation of dinitropropane species and their subsequent transformation into reaction products.

Supporting Pt + Cu on ZrPILC accelerates both stages (Table 1) as well as the rate of catalysis. Hence, though such key intermediates as isopropoxide and dinitropropane complexes are formed even without Pt and/or Cu, these active components

Table 1
Reactivity of the surface species and the steady-state rate of C_3H_6 NO_x SCR reaction for ZrPILC-based catalysts

Catalyst	T (°C)	Consumption rate constant of the surface complexes (min^{-1})		Rate of nitrate complexes consumption (molecules/min)[a]	Reaction rate (molecules/min)[a]
		Nitrate	Dinitropropane		
PILC	250	0.035	0.040	2×10^{18}	1.8×10^{18}
Pt,Cu/PILC	150	0.070	0.070	2.7×10^{18}	3×10^{18}

[a] Reaction mixture composition 0.2% NO + 0.2% C_3H_6 + 2.5% O_2 in N_2, IR flow cell, wafer density 10 mg/cm^2.

are clearly involved in formation of oxygenates and nitrite–nitrate species as well as in transformation of C,N,O-containing intermediates, especially as far as the redox stages are concerned [36].

4. Discussion

4.1. Specificity of the structure and texture of Zr-pillared clay-based catalysts as related to their high performance in realistic feeds

Detailed characterization of Zr-pillared clay-based catalysts with optimized structural and textural properties [12,13,19] revealed that they can be considered as nanostructured analogs of zeolitic systems.

Thus, simulation of high-resolution nitrogen adsorption isotherms by the Grand Canonical Monte Carlo method [19] revealed that for optimized preparation procedures, zirconia-pillared clays are characterized by an open structure of nanosized pillars comprised of either separate tetrameric units derived from the square polynuclear zirconium hydroxocomplex ($[Zr_4(\mu\text{-}OH)_8(OH)_8(H_2O)_8]$) ($Zr_4$) or their sheet-like dimers. In this structure, each pare of Zr cations is bound by two bridging hydroxyls (μ-OH). Within the galleries, these planar complexes are situated perpendicular to the aluminosilicate sheets being connected with them by the square vertexes. As the result, the gallery height in Zr-pillared clays is in the range of 0.8–0.9 nm corresponding to ultramicropores. A high specific surface area of micropores and developed mesoporosity (vide supra) ensures an easy access of long-chain hydrocarbons into the gallery space. Hence, the first factor making possible a high performance of catalysts based upon zirconia-pillared clays in the NO_x decane SCR is their favorable texture. Indeed, a large surface area and pore volume were demonstrated to be important for ensuring a higher activity of Pt/MCM-41 in NO_x HC SCR as compared with Pt/SiO_2 or Pt/Al_2O_3 [30].

An open structure of zirconia nanopillars, derived from that of Zr_4 tetramer, provides a plenty of bridging hydroxyls revealed by broad IR bands in the range of 3620–3740 cm^{-1} [12,13]. Neutralization of the excessive negative charge of aluminosilicate sheets by positively charged Zr_4 species completely suppresses the initial acidity of clays, as manifested by disappearance of bands at 3540–3615 cm^{-1} corresponding to hydroxyls bound with aluminosilicate layers [12,13]. The total acidity of Zr-pillared clays estimated by NH_3 TPD is much higher than that of the initial clay being proportional to the pillars density [37,38]. NH_3 TPD curves for ZrPILC are usually characterized by the maximum in the range of 250–300 °C with desorption continuing up to 500 °C [37–39]. This indicates the presence of both moderate and strong acid sites comparable by strength with those in H-ZSM-5 [40]. The amount of ammonia desorbing in the range of 80–500 °C is ∼0.7 mmol/g of clay [39], i.e. $\sim 4 \times 10^{20}$ molecules NH_3/g. At the typical values of the specific surface area of zirconia nanopillars ∼100 m^2/g of clay [11,19], this corresponds to approximately half a monolayer coverage of pillars by adsorbed ammonia molecules. Since the amount of Lewis acid sites probed by IR spectroscopy of adsorbed CO test molecules is very low (less than several % of Zr cations in the samples) [13], this means that regular bridging hydroxyls in zirconia nanopillars are indeed acidic. The IR spectra of adsorbed pyridine revealed bands at ∼1490, 1540 cm^{-1} and a shoulder of the IR band at 1638 cm^{-1} corresponding to Brönsted acid sites [37]. The presence of strong Brönsted acid sites in ZrPILC is directly confirmed by their ability to efficiently catalyze C-alkylation of phenol with methanol [41]. Sulfation increases the acidity of ZrPILC, thus improving their activity in acid-catalyzed reactions of 2-isopropanol dehydration to propene at 100 °C and *n*-hexane isomerization at 220 °C, being mixed with Pt/Al_2O_3 reforming catalyst in the latter case [39]. Hence, next factor apparently responsible for the high performance of ZrPILC-based catalysts in the NO_x SCR by decane, especially in feeds containing SO_2, is presence of rather strong Brönsted acid sites, which are able to efficiently activate alkanes, especially in combination with Pt. The positive effect of support acidity on the performance of Pt- or transition metal cations containing catalysts in NO_x HC SCR was reliably established [7,8,21,24,25,30,40,42].

The next factor of importance for the performance of ZrPILC could be neutralization of the excessive negative charge of aluminosilicate clay sheets by positively charged zirconium polynuclear hydroxocomplexes (pillars), making the external silica layers of these sheets non-reactive, similar to –Si–O–Si– fragments in zeolite walls. The hydrophobic nature of silica planes makes them suitable for the non-specific adsorption of long-chain hydrocarbons at moderate temperatures or even formation of liquid films within micropores at low temperatures. On the other hand, combination of positively charged nanopillars and negatively charged alumosilicate sheets provides required charge separation at their contact points favoring fixation of both cationic and anionic forms of ad-NO_x species or C,N,O-containing intermediates, being considered by Sachtler and co-workers [43,44] as important for the efficient performance of NO_x SCR catalysts.

At last, nanostructural specificity of ZrPILC affects the state of supported Cu cations and Pt, which certainly is of importance for these catalysts performance. Due to coordination unsaturation of bridging hydroxyls in Zr_4 complexes, they strongly interact with Cu cations ensuring their exclusive location on pillars as proved by EXAFS and ESR data [12,13]. Combination of UV–vis and FTIRS of adsorbed CO revealed that these cations are present as isolated species or Cu^+–Cu^{2+} dimers, while three-dimentional oxidic clusters typical for copper oxide supported on bulk zirconia and characterized by strong charge transfer band at ∼25 000 cm^{-1} are absent [12,13,27]. Hence, anchoring of copper cations by hydroxyls, as in zeolites, ensures their nearly atomic dispersion required for the high catalysts performance, while the ordered structure of nanopillars makes reproducibility of the properties of active/adsorption sites comparable with that in zeolites.

Such a strong interaction with bridging hydroxyls decreases the oxidation ability of supported Cu cations, which is reflected in the high-temperature shift of H_2 TPR peaks as compared

with those for Cu/bulk ZrO_2 samples (from ~200 to ~400–600 °C) [12,13]. This helps to avoid undesired combustion of hydrocarbons in NO_x SCR even at a high excess of oxygen in the feed. Such combustion is responsible for decreasing NO_x conversion into N_2 at high temperatures and generation of NO_2 [7,8,27].

Supporting of Pt was found to decrease the number of coordinatively unsaturated Cu^+/Cu^{2+} cations accessible to CO test molecules and bridging hydroxyls bound with Zr cations [12,13]. This suggests that Pt is also located on zirconia nanopillars being in part juxtaposed on Cu cations. As the result of interaction with Cu cations, Pt is in a partially oxidized state which is proved by IR band of adsorbed CO at ~2110 cm^{-1}, bands corresponding to CO adsorbed on Pt^0 particles were not revealed. Such an interaction between Pt and copper cations somewhat decreases stability of nitrates located on copper cations, shifting NO TPD peaks to lower temperatures [13].

Hence, from the structural and textural points of view, a high performance of Pt + Cu-loaded ZrPILC in the low-temperature range in realistic feeds is ensured by the same factors as for zeolitic systems with the important difference related to a high hydrothermal stability of ZrPILC.

4.2. Catalysts performance in realistic feeds and specificity of the reaction mechanism

For NO_x C_3H_6 SCR on ZrPILC-based catalysts, as revealed by FTIRS studies in dry feeds, main reaction route includes activation of propylene with participation of moderately acidic bridging hydroxyls thus forming isopropoxide complex. Its subsequent interaction with bridging or bidentate nitrates gives dinitropropane. The latter species is consumed by interaction with nitrate complexes giving N_2 via a sequence of acid–base and redox stages including formation of an efficient reductant—ammonia [20,36]. For ZrPILC by itself, due to a low reactivity of nitrates strongly bound with zirconia cations, as well as due to absence of sites able to efficiently perform redox stages (including the stage of NO oxidation to NO_2 required to generate surface nitrate species), catalytic activity is very low [13]. For Pt + Cu/ZrPILC, within the frames of the same mechanism, a high performance in C_3H_6 NO_x SCR in the low-temperature range is clearly determined by the action of mixed active component. Here, Pt is apparently involved in oxidation of NO into NO_2 thus accelerating the stage of nitrite–nitrates generation. Cu cations retain nitrite–nitrate species and ensure their high reactivity required for the efficient formation of organic nitrocompounds. Both Pt and Cu cations could be involved in such redox stages as transformation of dinitropropane (or β-nitropropylnitrite) into β-hydroxypropylamine via acid-catalyzed intermediate formation of β-hydroxypropynitrate [45]. Both redox and acidic function could be important for the stage of interaction between HNO_2 and β-hydroxypropylamine yielding acetone and N_2 [45]. Apparently, combustion of acetone is the most efficiently catalyzed by supported Pt.

In the high-temperature range, another NO_x HC SCR route operates for Pt + Cu-loaded ZrPILC, which includes interaction of acetate complex with nitrates yielding nitromethane adspecies [46]. The latter is transformed via sequence of parallel and consecutive steps such as those considered by Orlando et al. [3] and Chen et al. [44] yielding finally N_2 and deep oxidation products:

$$CH_3CHO \rightarrow CH_3COO^{\bullet} \rightarrow CH_2NO_2^{\bullet} \rightarrow O_2NCH_2NO_2^{-} \rightarrow NCO^{-} \rightarrow HNCO \rightarrow NH_3$$

$$NH_3 + HONO \rightarrow N_2 + 2H_2O$$

In this route, oxidative transformation of isopropoxide complexes into acetate species as well as the redox stage of nitromethane transformation into NCO are clearly catalyzed by Pt together with Cu. Transformation of acetates into nitromethane could be the acid-catalyzed reaction efficiently occurring on acid catalysts without any redox function [44].

All these routes leading to selective formation of N_2 in the excess of oxygen dominate only in the presence of Cu cations in the mixed active component (vide supra). Without Cu, a rather high selectivity of N_2O formation on Pt/ZrPILC even in humid feeds suggests operation of redox route [36] due to a high oxidation ability of supported Pt. Hence, the most important function of copper cations is to stabilize reactive nitrite–nitrate complexes involved in formation of organic nitrocompounds—key intermediates of NO_x HC SCR. Moreover, strong interaction of Pt atoms with copper cations makes them more oxidized thus decreasing their oxidation ability and preventing combustion of nitroorganics into products of deep oxidation and NO_x.

Hence, participation of nitrates and nitroorganic species in the rate-determining stage agrees with the mechanism of this reaction suggested for zeolite- or base oxide-supported transition metal cations and/or silver [20,36,45]. The key reaction intermediates such as nitrates, isopropoxide, nitroorganic compounds (dinitropropane, nitromethane), acetates are rather strongly bound species, which are retained by the surface sites in realistic feeds containing water and carbon dioxide. This apparently explains a weak or even positive effect of the surface hydroxylation or sulfation on the NO_x conversion. Indeed, surface hydroxylation or sulfation decreases the bonding strength and coverage of those species thus increasing their reactivity [17,18]. As compared with other systems, a unique feature of Zr-PILC-based catalysts is that activation of propylene involves neither Pt atoms/transition metal cations (Lewis acid sites) nor nitrates, which could be hampered by the surface hydroxylation and/or sulfation. In contrary, the increase of the Brönsted acidity of nanopillars due to their sulfation increases the rate of propylene activation into selective oxidation products, which is reflected in higher NO_x conversion. Hydroxylation and sulfation also suppress formation of nitrous oxide [21] usually associated with the specific function of Pt in HC SCR reactions [36].

Another factors could contribute to the high performance of Pt + Cu/ZrPILC catalysts in realistic feeds. First of all, they include an efficient oxidation of NO into NO_2 catalyzed by Pt even in wet feeds, which is required for the fast generation of key intermediates—ad-NO_x species. Moreover, for these

systems in wet feeds, as revealed by NO_x TPD, formation of an important intermediate—nitrous acid considered to be involved in N–N pairing [2,44] appears to be facilitated (vide supra).

Presence of water in the feed is proved to accelerate hydrolysis of important intermediates such as amines [47], isocyanates [44], etc. through the acid-catalyzed stages, which seems to be also important for enhanced performance of our catalysts in realistic feeds.

More traditional reason for the enhanced activity of microporous catalysts in realistic feeds is suppression of the surface blocking by a variety of polymeric species formed due to condensation/polymerization of aldehydes [2], isocyanates [36], etc.

Enhanced performance of ZrPILC-based catalysts in realistic feeds observed for decane NO_x SCR suggests operation of similar factors considered above as related to the mechanism of C_3H_6 SCR. Apparently, Pt action here is to ensure complete/partial oxidation [8] and cracking of decane [48,49] which is promoted by the ZrPILC acidity enhanced due to sulfation (vide supra). For sulfated zirconia systems doped with transition metal cations formation of olefins due to dehydrogenation of alkanes is possible even at temperatures ~200 °C [48,49]. Olefins can be formed on sulfated ZrPILC even at lower (~100 °C) temperatures via dehydration of oxygenates such as propanol, etc. [39]. As the result, mechanistic features for the reactions of NO_x SCR by propylene and decane can be in fact similar. Moreover, even for Rh-promoted Ag/Al_2O_3 catalyst, the results of mechanistic FTIR studies of Sato et al. [5] for decane NO_x SCR agree with the general schemes of propylene SCR including formation of oxygenates, their transformation into organic nitrocompounds by interaction with the surface nitrate species followed by their transformation into isocyanates, amines and, finally, nitrogen. In the work of Eränen et al. [47], for Ag/alumina catalyst, a similar sequence of steps was suggested for this reaction, being supplemented with the important conclusion that interaction between ammonia, amine and NO_x species can proceed in the gas phase as well. However, at temperatures ~150 °C, for long-chain hydrocarbons such as decane, another route can operate as well including interaction of NO_x with olefins "dissolved" in the polymolecular hydrocarbon layers covering the hydrophobic silica planes within the galleries of pillared clay. This well-known liquid phase reaction occurring even at room temperature was studied in details by Brown [50]. For the case of isobutene, its reaction with NO_2 produces 1-nitro-*tert*-butyl radical. The radical reacts with nitric oxide to form 1-nitro-2-nitroso-isobutane. This compound can react with two NO molecules forming unstable *N*-nitrosonitrite derivative rapidly decomposing to 1-nitro-*tert*-butyl radical, nitrogen and the NO_3 radical. The latter reacts with NO molecule to form two molecules of NO_2, thus closing the cycle. In our case, nitroorganic compounds could migrate to hydrophilic zirconia pillars. Here, they can be converted into N_2 and deep oxidation products via routes similar to those considered above or through a route suggested by Smith and Iwasawa [51] for the C_3H_6 NO_x SCR based on the considered above liquid-phase chemistry including possible formation of 1,2-dinitropropane. Such a biphasic scheme of NO_x HC SCR reaction with participation of long-chain hydrocarbons, though rather speculative at present and requiring more detailed studies of the reaction stoichiometry at low temperatures, could indeed explain observed high performance of Pt + Cu/ZrPILC catalysts in the low-temperature range. Its realization certainly requires specificity of the nanostructure of ZrPILC considered above, a synergy of Pt and acid sites action in producing olefins at low temperatures as well as a high density and uniformity of zirconia nanopillars spatial distribution within galleries to ensure a short diffusion path for the olefins and nitroorganic redistribution between the liquid hydrocarbon film and pillars. In general, the concept of bi-phasic (bifunctional) catalysts comprised, i.e., of acidic zeolites and oxides able to oxidize NO into NO_2 first demonstrated by Yokoyama and Misono [52] appears to be rather promising. The latest example demonstrates a unique water-enhanced low-temperature activity of ceria-coated Cu-ZSM-5 in the NO_x propylene SCR with a maximum of activity reached at ~250 °C [53].

5. Conclusion

Pt + Cu-loaded zirconia-pillared clays demonstrate a high performance in the NO_x SCR by decane and propylene in the presence of SO_2 and water, which makes them promising for the diesel exhaust after-treatment. The factors determining such a high performance are in general associated with the specificity of these interlayer catalysts nanostructural arrangement, making them similar to zeolite-like systems. This includes developed micro- and mesoporosity, moderate acidity of bridging hydroxyls bound with Zr cations in nanopillars and a high dispersion of supported Pt + Cu active component along with its moderate HC combustion ability. The scheme of the NO_x HC SCR reaction mechanism includes steps with participation of strongly bound intermediates which are either accelerated or insensitive to the presence of water and SO_2 in the feed. Combination of Pt and Cu in the active component allows to ensure domination of the reaction route with a high N_2 selectivity typical for copper-containing catalysts while maintaining a high level of the low-temperature activity typical for supported Pt catalysts. Suppression of the catalysts coking in the real feeds is also important.

Acknowledgements

This work was in part supported by INTAS 97-11720 Project and Integration Project 8.23 of Presidium RAS.

References

[1] M. Iwamoto, Stud. Surf. Sci. Catal. 130 (2000) 23.
[2] B. Wen, Y.H. Yeom, E. Weitz, W.M.H. Sachtler, Appl. Catal. B: Environ. 48 (2004) 125.
[3] Th.M. Orlando, A. Alexandrov, A. Lebsack, J. Herring, J.-W. Hoard, Catal. Today 89 (2004) 151.
[4] M. Shelef, Chem. Rev. 95 (1995) 209.
[5] K. Sato, T. Yoshinari, Y. Kintaichi, M. Haneda, H. Hamada, Appl. Catal. B: Environ. 44 (2003) 67.

[6] G. Corro, J.L.G. Fierro, R. Montiel, S. Castillo, M. Moran, Appl. Catal. B: Environ. 46 (2003) 307.
[7] F. Figueras, B. Coq, E. Ensuque, D. Tachon, G. Delahay, Catal. Today 42 (1998) 117.
[8] G. Delahay, E. Ensuque, B. Coq, F. Figueras, J. Catal. 175 (1998) 7.
[9] C.E. Quincoces, S. Guerrero, P. Araya, M.G. Gonzalez, Catal. Commun. 6 (2005) 75.
[10] R.T. Yang, N. Trappiwattanannon, R.Q. Long, Appl. Catal. B: Environ. 19 (1998) 289.
[11] V.B. Fenelonov, A.Yu. Derevyankin, V.A. Sadykov, Microp. Mesop. Mater. 47 (2001) 359.
[12] V.A. Sadykov, T.G. Kuznetsova, V.P. Doronin, T.P. Sorokina, G.M. Alikina, D.I. Kochubei, B.N. Novgorodov, E.A. Paukshtis, V.B. Fenelonov, V.I. Zaikovskii, V.A. Rogov, V.F. Anufrienko, N.T. Vasenin, V.A. Matyshak, G.A. Konin, A.Ya. Rozovskii, V.F. Tretyakov, T.N. Burdeynaya, J.R.H. Ross, J.P. Breen, Chem. Sustain. Dev. 11 (2003) 249.
[13] V.A. Sadykov, T.G. Kuznetsova, V.P. Doronin, E.M. Moroz, D.A. Ziuzin, D.I. Kochubei, B.N. Novgorodov, V.N. Kolomiichuk, G.M. Alikina, R.V. Bunina, E.A. Paukshtis, V.B. Fenelonov, O.B. Lapina, I.V. Yudaev, N.V. Mezentseva, A.M. Volodin, V.A. Matyshak, V.V. Lunin, A.Ya. Rozovskii, V.F. Tretyakov, T.N. Burdeynaya, J.R.H. Ross, Top. Catal. 32 (2005) 29.
[14] G.A. Konin, A.N. Il'ichev, V.A. Matyshak, T.I. Khomenko, V.N. Korchak, V.A. Sadykov, V.P. Doronin, R.V. Bunina, G.M. Alikina, T.G. Kuznetsova, E.A. Paukshtis, V.B. Fenelonov, V.I. Zaikovskii, A.S. Ivanova, S.A. Beloshapkin, A.Ya. Rozovskii, V.F. Tretyakov, J.R.H. Ross, J.P. Breen, Top. Catal. 17 (2001) 193.
[15] V.A. Sadykov, V.V. Lunin, A.Ya. Rozovskii, V.A. Matyshak, in: V.V. Lunin, P. Tundo, E.S. Lokteva (Eds.), Green Chemistry in Russia, INCA, Venezia, Italy, 2005, p. 45.
[16] N. Li, A. Wang, X. Wang, M. Zheng, R. Cheng, T. Zhang, Appl. Catal. B: Environ. 48 (2004) 259.
[17] M. Kantcheva, A.S. Vakkasoglu, J. Catal. 223 (2004) 364.
[18] B. Tsyntsarski, V. Avreyska, H. Kolev, Ts. Marinova, D. Klissurski, K. Hadjiivanov, J. Mol. Catal. 193 (2003) 139.
[19] D. Efremov, V. Doronin, T. Kuznetsova, V. Sadykov, J. Phys. Chem. B 109 (2005) 7451.
[20] V.A. Sadykov, V.V. Lunin, V.A. Matyshak, E.A. Paukshtis, A.Ya. Rozovskii, N.N. Bulgakov, J.R.H. Ross, Kinet. Catal. 44 (2003) 379.
[21] V.A. Sadykov, R.V. Bunina, G.M. Alikina, A.S. Ivanova, T.G. Kuznetsova, S.A. Beloshapkin, V.A. Matyshak, G.A. Konin, A.Ya. Rozovskii, V.F. Tretyakov, T.N. Burdeynaya, M.N. Davydova, J.R.H. Ross, J.P. Breen, J. Catal. 200 (2001) 131.
[22] G.A. Konin, A.N. Il'ichev, V.A. Matyshak, T.I. Khomenko, V.N. Korchak, V.A. Sadykov, V.P. Doronin, R.V. Bunina, G.M. Alikina, T.G. Kuznetsova, E.A. Paukshtis, V.B. Fenelonov, V.I. Zaikovskii, A.S. Ivanova, S.A. Beloshapkin, A.Ya. Rozovskii, V.F. Tretyakov, J.R.H. Ross, J.P. Breen, Top. Catal. 16/17 (2001) 193.
[23] G. Zhang, T. Yamaguchi, H. Kawakami, T. Suzuki, Appl. Catal. B: Environ. 1 (1992) L15.
[24] M. Kantcheva, E.Z. Ciftlikli, J. Phys. Chem. B 106 (2002) 3941.
[25] M. Kantcheva, A.S. Vakkasoglu, J. Catal. 223 (2004) 352.
[26] V. Indovina, D. Pietrogiacomi, M.C. Campa, Appl. Catal. B: Environ. 39 (2002) 115.
[27] J. Pasel, V. Speer, Ch. Albrecht, F. Richter, H. Papp, Appl. Catal. B: Environ. 25 (2000) 105.
[28] V.A. Matyshak, O.V. Krylov, Catal. Today 25 (1995) 1.
[29] R. Burch, J.P. Breen, F.C. Meunier, Appl. Catal. B: Environ. 39 (2002) 283.
[30] S.-C. Shen, S. Kawi, Appl. Catal. B: Environ. 45 (2003) 63.
[31] V.A. Sadykov, R.V. Bunina, G.M. Alikina, V.P. Doronin, T.P. Sorokina, D.I. Kochubei, B.N. Novgorodov, E.A. Paukshtis, V.B. Fenelonov, Yu. Derevyankin, A.S. Ivanova, V.I. Zaikovskii, T.G. Kuznetsova, S.A. Beloshapkin, V.N. Kolomiichuk, L.M. Plasova, V.A. Matyshak, A. Konin, Ya. Rozovskii, V.F. Tretyakov, T.N. Burdeynaya, M.N. Davydova, J.R.H. Ross, J.P. Breen, F.C. Meunier, Mater. Res. Soc. Symp. Proc. 581 (2000) 435.
[32] V.A. Sadykov, S.L. Baron, V.A. Matyshak, G.M. Alikina, R.V. Bunina, A.Ya. Rozovskii, V.V. Lunin, E.V. Lunina, A.N. Kharlanov, A.S. Ivanova, S.A. Veniaminov, Catal. Lett. 37 (1996) 157.
[33] Q. Sun, Z.X. Gao, H.Y. Chen, W.M.H. Sachtler, J. Catal. 201 (2001) 89.
[34] A.A. Davydov, Infrared Spectroscopy of Adsorbed Species on the Surface of Transition Metal Oxides, Wiley, New York, 1990.
[35] T.Ya. Paperno, V.V. Perkalin, Infrared Spectra of Nitro Compounds, LSU, Leningrad, 1974.
[36] R. Burch, Catal. Rev. 46 (2004) 271.
[37] H.J. Chae, I.-S. Nam, S.W. Ham, S.B. Hong, Catal. Today 68 (2001) 31.
[38] P. Canizares, J.L. Valverde, M.R. Sun Kou, C.B. Molina, Microp. Mesop. Mater. 29 (1999) 267.
[39] S.B. Caabene, L. Bergaoui, A. Ghorbel, J.F. Lambert, P. Grange, Appl. Catal. A: Gen. 252 (2003) 411.
[40] K. Krishna, M. Makkee, Appl. Catal. B: Environ. 59 (2005) 35.
[41] B.G. Mishra, G.R. Rao, Microp. Mesop. Mater. 70 (2004) 43.
[42] H.H. Ingelsten, M. Skoglundh, E. Fridell, Appl. Catal. B: Environ. 41 (2003) 287.
[43] Y.-H. Yeom, B. Wen, W.M.H. Sachtler, E. Weitz, J. Phys. Chem. B 298 (2004) 5386.
[44] H.-Y. Chen, Q. Sun, B. Wen, Y.-H. Yeom, E. Weitz, W.M.H. Sachtler, Catal. Today 96 (2004) 1.
[45] J.A. Martens, A. Cauvel, A. Francis, C. Hermans, F. Jayat, M. Remy, M. Keung, J. Lievens, P.A. Jacobs, Angew. Chem. Int. Ed. Eng. 37 (1998) 1901.
[46] K.A. Chernyshov, Ph.D. Thesis, Moscow Textiles State University, 2005.
[47] K. Eränen, F. Klingstedt, K. Arve, L.-E. Lindfors, D.Yu. Murzin, J. Catal. 227 (2004) 328.
[48] T.-K. Cheung, B.C. Gates, Top. Catal. 6 (1998) 41.
[49] Z. Hong, K.B. Fogash, J.A. Dumesic, Catal. Today 51 (1999) 269.
[50] J.F. Brown, J. Am. Chem. Soc. 79 (1957) 2480.
[51] R. Smits, Y. Iwasawa, Appl. Catal. 6 (1995) L201.
[52] Ch. Yokoyama, M. Misono, Catal. Lett. 29 (1994) 1.
[53] M.K. Neylon, M.J. Castagnola, N.B. Castagnola, C.L. Marshall, Catal. Today 96 (2004) 53.